Hydrothermal Synthesis and Characterization of Two New Microporous Zinc-Substituted Gallium Phosphates Templated by Diaminocyclohexane: $(H_2DACH)_2[Zn_4Ga_2(HPO_4)_3(PO_4)_4]$ and $(H_2DACH)[Zn_2Ga_2(PO_4)_4]$

Chia-Her Lin and Sue-Lein Wang*

Department of Chemistry, National Tsing Hua University, Hsinchu, Taiwan 300

Received May 16, 2000. Revised Manuscript Received August 25, 2000

Two new zinc-substituted gallophosphates, $(H_2DACH)_2[Zn_4Ga_2(HPO_4)_3(PO_4)_4]$ (**1**) and $(H_2DACH)[Zn_2Ga_2(PO_4)_4]$ (**2**), have been synthesized under mild hydrothermal conditions and characterized by single-crystal X-ray diffraction, solid-state NMR spectroscopy, and thermogravimetric analysis. Both structures are built up with MO_4 (M = Zn, Ga) and PO_4 (or HPO_4) tetrahedra. Compound **1** adopts a novel microporous framework which contains the highest transition-metal concentration of any MGaPO. The structure may be viewed as stacking of $[Zn_2Ga(HPO_4)_2(PO_4)_2]_2$ layers along *a* linked by extra HPO_4 tetrahedra as pillars to generate intersecting 12-ring channels with dimensions ~8.1 × 8.1 Å. Compound **2** has a CGS framework topology but a higher divalent-metal content than the isostructural materials of $(C_7NH_{14})[MGa_3P_4O_{12}]$ (M = Co, Zn). Diprotonated 1,2-diaminocyclohexane (DACH) cations are ordered at the intersections of two interconnected channels in both **1** and **2**. They represent the first zinc-substituted gallophosphate templated by dibasic amine and showing distinguishable Zn sites. The solid-state ^{31}P MAS NMR spectrum of **1** showed a resonance for the HPO_4^{2-} group that was shifted downfield by ~8 ppm relative to the PO_4^{3-} group. On the basis of the results of TG/DT analyses, both frameworks can be thermally stable up to ~300 °C. Crystal data: **1**, monoclinic, *C*2/*c*, $a = 23.568(1)$ Å, $b = 10.242(1)$ Å, $c = 16.235(1)$ Å, $\beta = 108.115(1)°$, $Z = 4$; **2**, monoclinic, $P2_1/c$, $a = 14.320(1)$ Å, $b = 16.255(1)$ Å, $c = 8.855(1)$ Å, $\beta = 90.134(1)°$, $Z = 4$.

Introduction

Metal silicates and phosphates that possess channels, cavities, or cages with aperture diameters in the range of 3−14 Å offer good means for designing or modifying new inorganic heterogeneous catalysts.[1−3] The search for new framework topology of such highly porous materials has been extremely active in recent years.[4,5] One particular area is the synthesis and characterization of open-framework gallium phosphates, which have attracted much attention since the report of the very first compound, $(^iPrNH_3)[Ga_4(PO_4)_4(OH)]\cdot H_2O$,[6] with a structure similar to those of the AlPO-*n* family and the discovery of cloverite,[7] a much noted GaPO phase for its unique framework containing a supercage of ~30 Å. Following the intensive study of heteroatom-substituted AlPOs,[8,9] incorporation of transition metal (TM) ions into the GaPO framework has started to emerge.[10−12] The driving force behind the effort is not only to offer the possibility of understanding the location and environment of the TM ion sites, which are still ambiguous for most MAlPO materials, but also to engineer new open frameworks with desired chemical and physical properties. Recently we have combined hydrothermal conditions with large inorganic cation or dibasic amine molecules as the structure-directing reagents and successfully prepared a few open-framework transition-metal arsenates and phosphates.[13−15] As not many TM-substituted gallium phosphates were characterized and most of them were prepared from gels, we thought to explore the possibility of direct synthesis of new MGaPO materials via mild hydrothermal routes. Our efforts resulted in the preparation of two unique MnGaPO frameworks, $(C_4H_{10}N_2)_2Mn^{II}Mn^{III}Ga_5(H_2O)(PO_4)_8$[16] and $Mn_3(H_2O)_6Ga_4(PO_4)_6$.[17] Recently, we have extended our

(1) Thomas, J. M. *Angew Chem.; Int. Ed. Engl.* **1988**, *27*, 1673.
(2) Ying, J. Y.; Wong,, M. S. *Angew. Chem., Int. Ed.* **1999**, *38*, 56.
(3) Wilson, S. T.; Lok, B. M.; Messing, C. A.; Cannan, T. R.; Flanigen, E. M. *J. Am. Chem. Soc.* **1982**, *104*, 1146.
(4) Cheetham, A. K.; Ferey, G.; Loiseau, T. *Angew. Chem., Int. Ed.* **1999**, *38*, 3268.
(5) Xiao, F. S.; Qiu, S.; Pang, W.; Xu, R. *Adv. Mater.* **1999**, *11*, 1091.
(6) Parise, J. B. *J. Chem. Soc., Chem. Commun.* **1985**, 606.
(7) Estermann, M.; McCusker, L. B.; Baerlocher, C.; Merrouche, A.; Kessler, H. *Nature* **1991**, *352*, 320.
(8) Davis, M. E. *Microporous Mesoporous Mater.* **1998**, *21*, 173.
(9) Hartmann, M.; Kevan, L. *Chem. Rev.* **1999**, *99*, 635.
(10) Chippindale, A. M.; Walton, R. I. *J. Chem. Soc., Chem. Commun.* **1994**, 2453.
(11) Bu, X.; Feng, P.; Stucky, G. D. *Science* **1997**, *278*, 2080.
(12) Chippindale, A. M.; Cowley, A. R. *Microporous Mesoporous Mater.* **1998**, *21*, 271.
(13) Lii, K. H.; Huang, Y. F.; Zima, V.; Huang, C. Y.; Lin, H. M.; Jiang, Y. C.; Liao, F. L.; Wang, S. L. *Chem. Mater.* **1998**, *10*, 2599.
(14) Hsu, K. F.; Wang, S. L. *Inorg. Chem.* **1998**, *37*, 3230.
(15) Hsu, K. F.; Wang, S. L. *Chem. Mater.* **1999**, *11*, 1876.
(16) Hsu, K. F.; Wang, S. L. *Chem. Commun.* **2000**, 135.
(17) Hsu, K. F.; Wang, S. L. *Inorg. Chem.* **2000**, *39*, 1773.

10.1021/cm000399q CCC: $19.00
Published on Web 11/23/2000

investigation to the Zn/Ga/P/O system with the dibasic 1,2-diaminocyclohexane (DACH) as the template molecule. Herein we report two new ZnGaPOs: $(H_2DACH)_2[Zn_4Ga_2(HPO_4)_3(PO_4)_4]$ (**1**), a novel porous framework containing intersecting 12-ring channels with dimensions ~8.1 × 8.1 Å and void space ~39.4% of cell volume, and $(H_2DACH)Zn_2Ga_2(PO_4)_4$ (**2**), the second ZnGaPO with CGS (IZA designation) topology.[18] The syntheses, crystal structures, solid-state ^{31}P and ^{71}Ga MAS NMR data, and thermal analyses of the title compounds are presented and discussed.

Experimental Section

Synthesis and Compositional Analysis. Chemicals of reagent grade or better were used as received. Hydrothermal reactions were carried out in Teflon-lined digestion bombs with an internal volume of 23 mL under autogenous pressure by heating the reaction mixtures at 150 °C for 2 d followed by slow cooling at 5 °C h^{-1} to room temperature. Transparent colorless crystals in two different morphology, lamellar and columnar, together with a tiny amount of black solid were obtained by heating a mixture of DACH[19] (1.1 mL, 9.0 mmol), $ZnCl_2$ (0.4089 g, 3.0 mmol), Ga_2O_3 (0.2812 g, 1.5 mmol), 3 M H_3PO_4 (2.0 mL, 6.0 mmol), ethylene glycol (EG) (8 mL), and H_2O (2 mL) with an initial pH value of 2.6. The lamellar-shaped crystals (yield of ~10%) were $[H_2DACH]_2[Zn_4Ga_2(PO_4)_4(HPO_4)_3]$ (**1**) and the columnar-shaped (yield of ~90%) were $[H_2DACH][Zn_2Ga_2(PO_4)_4]$ (**2**) as determined by single-crystal X-ray diffraction (vide infra). The yield of **1** could be raised to ~30% by changing the solvent system to a mixture of 5 mL of EG and 5 mL of H_2O (5 mL). Later, single-phase **2** was prepared by heating the mixture of DACH (0.368 mL, 3.0 mmol), $ZnCl_2$ (0.2726 g, 2.0 mmol), $Ga(NO_3)_3{\cdot}xH_2O$ (0.2557 g, 1.0 mmol), 3 M H_3PO_4(2.0 mL, 6.0 mmol), EG (5.0 mL), and H_2O (5.0 mL) with an initial pH value of ~2.2. The source of Ga atom as well as the retention time of reaction (vide infra) played important roles in preparing single-phased product of **2**. Attempts to prepare the pure phase of **1** have not been successful. To all experiments was added 0.05 mL of $Si(OEt)_4$ as a mineralizer, and dilute HCl (3 M) was used to adjust the pH. Powder X-ray diffraction patterns measured on manually selected crystals of these materials confirmed phase purity before chemical and spectroscopic analyses were performed.

Elemental analysis was carried out to confirm organic contents. Anal. found for **1**: C, 10.98; N, 3.88; H, 2.70. Calcd: C, 11.08; N, 4.31; H, 2.71. Anal. found for **2**: C, 9.18; N, 3.54; H, 2.16. Calcd: C, 9.40; N, 3.66; H, 2.10. The atomic ratio of Zn to Ga determined from single-crystal structure refinements (2:1 for **1** and 1:1 for **2**) was further confirmed by electron probe microanalysis data (2.06:1 for **1** and 1.01:1 for **2**).

Single-Crystal X-ray Structure Analysis. Two crystals of dimensions 0.05 × 0.20 × 0.50 mm of **1**, and 0.10 × 0.20 × 0.20 mm for **2** were selected for indexing and intensity data collection. The diffraction measurements were performed on a Siemens Smart-CCD diffractometer system equipped with a normal focus, 3 kW sealed-tube X-ray source (λ = 0.71073 Å). Intensity data were collected in 1271 frames with increasing ω (width of 0.3° per frame). Unit cell dimensions were determined by a least-squares fit of 5078 reflections for **1** and 6303 reflections for **2**. The intensity data were corrected for *Lp* and absorption effects. The absorption correction was based on symmetry-equivalent reflections using the SADABS program.[20] On the basis of systematic absences and statistics of intensity distribution, the space groups were determined to be *C*2/*c* for **1** and $P2_1/c$ for **2**. Number of measured and observed reflections ($I_{obs} > 3\sigma_I$) are 9366 and 7271 for **1** and 12 721 and 9527 for **2**. Direct methods were used to locate the Ga (or Zn), P, and a few oxygen atoms with the remaining non-hydrogen atoms found from successive difference maps. As the atomic scattering factors are too similar, it was not possible to distinguish the Zn from the Ga sites in structure refinements. Since the bond length for Zn−O is significantly longer than that for Ga−O, the results of bond-valence sum calculation[21] were used to determine the type of metal sites. All meal sites except that of Zn(1) in **1** and Zn(1) and Ga(2) in **2** were occupied by mixed Zn and Ga atoms. The hydroxo oxygen atoms, O(12) and O(14), in **1** were identified by referring to their bond-valence sums as well. H atoms were calculated using a riding model. Structural parameters were refined on the basis of F^2. The final cycle of refinements, including the atomic coordinates and anisotropic thermal parameters for all non-hydrogen atoms and fixed atomic coordinates and isotropic thermal parameters for H atoms, converged at R = 0.0423 for **1**, and R = 0.0433 for **2**. Corrections for secondary extinction and anomalous dispersion were applied. Neutral-atom scattering factors for all atoms were taken from the standard sources. All calculations were performed by using SHELXTL programs.[22] The crystallographic data are given in Table 1.

Table 1. Crystallographic Data for Compounds 1, and 2

	1	**2**
formula	$C_{12}H_{35}Ga_2N_4O_{28}P_7Zn_4$	$C_6H_{16}Ga_2N_2O_{16}P_4Zn_2$
fw	1301.23	766.27
space group	*C*2/*c*	$P2_1/c$
a, Å	23.568(2)	14.320(1)
b, Å	10.242(1)	16.255(1)
c, Å	16.235(1)	8.855(1)
β, deg	108.115(1)	90.134(1)
volume, Å^3	3724.4(4)	2061.2(2)
Z	4	4
no. refltn collected	9366 (7271 > 3σ(*I*))	12457 (9527 > 3σ(*I*))
D_{calcd}, g cm^{-3}	2.245	2.469
μ, mm^{-1}	4.430	5.278
T, °C	22	22
λ, Å	0.71073	0.71073
R1[a]	0.0423	0.0433
*w*R2[b]	0.1247	0.1307

[a] $R1 = \sum||F_o| - |F_c||/\sum|F_o|$. [b] $wR2 = [\sum w(|F_o|^2 - |F_c|^2)^2]/\sum w(|F_o|^2)^2]^{1/2}$, $w = [\sigma^2(F_o^2) + 0.0630P]^2 + 35.67P]$ for **1**, and $w = [\sigma^2(F_o^2) + 0.0564P]^2 + 9.95P]$ for **2**.

Thermogravimetric Analysis. Thermal analyses (TGA/DTA), using a Seiko TG/DTA 300 analyzer, were performed on powder samples of **1** (5.00 mg) and **2** (7.56 mg) under flowing N_2 with a heating rate of 10 °C min^{-1}. As indicated by the TGA/DTA curves shown in Figure 1, both compounds were thermally stable up to ~300 °C and revealed a mass loss over the range 300−550 °C. The stage should correspond to the dehydration of HPO_4^{2-} groups (calcd 2.07% for 1) and the removal of organic contents (calcd 17.48% for **1** and 14.87% for **2**). However, the observed mass losses were much lower than the expected, i.e., 18.2 vs 19.55% for **1** and 12.5 vs 14.8% for **2**. The lower reduction in mass loss was likely due to the retention of carbon in the solid residues, since they turned black on heating. Beyond 800 °C, the black solid residue of **1** showed a further mass loss and became bleached at 1000 °C, indicating that the residual carbon was removed.

Solid-State NMR Measurements. ^{71}Ga and ^{31}P MAS NMR spectra were collected on a Bruker DSX 400 spectrometer equipped with a standard Bruker 4-mm MAS probe head at 9.4 T. Sample spinning speeds of 12 kHz for Ga and 7 kHz for P were applied. Chemical shifts were respectively reported relative to 1.0 M $Ga(NO_3)_3$ and 85% H_3PO_4 solutions as external references. The ^{31}P NMR spectra showed two broad peaks respectively centered at 5.4 and −2.5 ppm for **1** and one

(18) Cowley, A. R.; Chippindale, A. M. *Microporous Mesoporous Mater.* **1999**, *28*, 163.

(19) The chemical used is a mixture of cis and trans isomers of 1,2-diaminocyclohexane.

(20) Sheldrick, G. M. *SADABS*; Siemens Analytical X-ray Instrument Division: Madison, WI, 1998.

(21) Brown, I. D.; Altermann, D. *Acta Crystallogr.* **1985**, *B41*, 244.

(22) Sheldrick, G. M. *SHELXTL Programs*, Release Version 5.1; Bruker AXS, 1998.

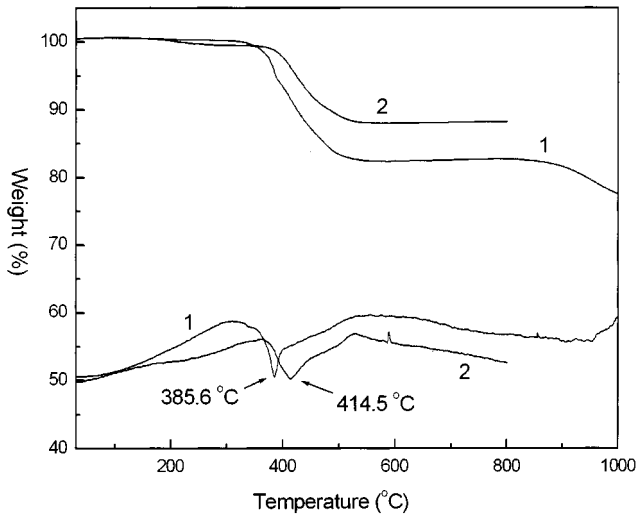

Figure 1. TGA (top) and DTA (bottom) curves for $(H_2DACH)_2[Zn_4Ga_2(HPO_4)_3(PO_4)_4]$ (**1**) and $(H_2DACH)[Zn_2Ga_2(PO_4)_4]$ (**2**) in flowing N_2 at 10 °C min^{-1}.

peak at −2.8 ppm for **2**. The ^{71}Ga MAS NMR spectra showed one single peak at 113 ppm for **1** and 119 ppm for **2**.

Results and Discussion

The atomic coordinates, thermal parameters, and bond distances are given in Tables 2 and 3, respectively. Compound **1** is comprised of MO_4 (M = Zn and Ga), HPO_4, and PO_4 tetrahedra. They share corners to form an open network with large channels occupied by diprotonated *trans*-1,2-diaminohenane molecules. Projections of the three-dimensional structure are shown in Figure 2. The most striking feature of **1** is the possession of two-dimensional 12-ring channels with ~8.1 Å × 8.1 Å openings (Figure 3). The large tunnels also exhibit lateral 6-ring and 8-ring windows along [110] and [011]. Big cages, each defined by six 12-membered rings and accommodating two H_2DACH^{2+} cations, can be located at the channel intersections. The tremendously voided space not occupied by the framework atoms can be estimated by PLATON analysis.[23] The result showed that 1473.5 $Å^3$ (ca. 39.6% of a unit cell volume) was to be "solvent accessible". Excluding zeolite structures, open metal phosphate frameworks containing multidimensional 12-ring channels are scarcely found to date. Compound **1** is believed to be the first example possessing two-dimensional 12-ring channels in the M/Ga/P/O system.

The porous structure of **1** may be alternatively viewed as stacking of the $[Zn_2Ga(HPO_4)(PO_4)_2]_2$ layers along the *a*-axis with $HP(4)O_4$ tetrahedra as pillars. As depicted in Figure 4, the thick tetrahedral layer is built up from $4^76^28^2$ cages. They interconnect via common vertexes to generate a 2D porous network with 8-ring openings toward the [011] direction. The interlayer $HP(4)O_4$ groups are disordered into two sites near 2-fold rotation axes. The H_2DACH^{2+} cations reside in the channels enclosed by adjacent layers and $HP(4)O_4$ tetrahedra. No H bonds were found between the organic cations and the pillaring $HP(4)O_4$ or intralayered PO_4 tetrahedra. However, weak H-bonding interaction may exist between the intralayered $HP(3)O_4$ and H_2DACH^{2+} cations, due to the short contact of 2.845 Å between N(1) and O(12).

(23) Spek, L. *Acta Crystallogr. Sect. A*, **1990**, *46*, C34.

Table 2. Atomic Coordinates (×10⁴) and Thermal Parameters (Å² × 10³) for (1) and (2)

atom	*x*	*y*	*z*	U_{eq}[a]
		Compound **1**		
Ga(1)[b]	2980(1)	908(1)	245(1)	27(1)
Zn(1)	3774(1)	−5567(1)	6091(1)	26(1)
Zn(2)[c]	3021(1)	−2539(1)	2776(1)	25(1)
P(1)	2666(1)	−5127(1)	1755(1)	25(1)
P(2)	3307(1)	−3472(1)	4633(1)	24(1)
P(3)	3342(1)	−1655(1)	1163(1)	28(1)
P(4)[d]	5009(1)	−6235(4)	7540(1)	41(1)
P(4)[d]	4825(7)	−5870(19)	7888(10)	41(1)
O(1)	2514(2)	−3907(4)	2183(3)	36(1)
O(2)	2775(2)	164(4)	−841(3)	47(1)
O(3)	2409(2)	−1330(4)	2729(3)	37(1)
O(4)	3312(2)	−4892(5)	6772(3)	50(1)
O(5)	3517(2)	−3035(4)	3872(2)	37(1)
O(6)	3645(2)	−4720(4)	4993(3)	39(1)
O(7)	2371(2)	1306(4)	714(3)	38(1)
O(8)	3442(2)	2427(3)	342(2)	35(1)
O(9)	3523(2)	−1898(4)	2147(2)	35(1)
O(10)	3502(2)	−244(3)	1021(2)	32(1)
O(11)	3679(2)	−7408(4)	5758(3)	42(1)
O(12)	2665(2)	−1872(4)	740(3)	43(1)
O(13)	4586(2)	−5422(6)	6809(4)	68(2)
O(14)	4658(3)	−7161(9)	7926(5)	107(3)
N(1)	3439(3)	−2796(9)	8920(4)	75(2)
N(2)	3514(4)	−1749(12)	7286(6)	113(4)
C(1)	3968(4)	−2761(15)	8644(8)	150(8)
C(2)	3976(6)	−1569(17)	8112(7)	218(13)
C(3)	4552(8)	−830(20)	8400(20)	420(30)
C(4)	5018(7)	−1390(20)	9174(16)	251(13)
C(5)	4834(14)	−2660(20)	9477(15)	300(20)
C(6)	4446(8)	−3760(18)	9007(17)	590(60)
		Compound **2**		
Ga(1)[b]	9732(1)	1291(1)	5868(1)	19(1)
Ga(2)	14635(1)	2298(1)	8656(1)	31(1)
Zn(1)	11316(1)	1615(1)	11907(1)	21(1)
Zn(2)[c]	13647(1)	382(1)	4219(1)	26(1)
P(1)	11376(1)	313(1)	4474(2)	17(1)
P(2)	10253(1)	2123(1)	8880(2)	18(1)
P(3)	15275(1)	1314(1)	5880(2)	26(1)
P(4)	13549(1)	1530(1)	11466(2)	27(1)
O(1)	10823(3)	666(3)	5814(5)	27(1)
O(2)	10979(3)	631(3)	12988(5)	31(1)
O(3)	11307(3)	−632(2)	4524(5)	28(1)
O(4)	12385(3)	567(3)	4734(6)	33(1)
O(5)	10533(3)	1530(3)	10141(5)	33(1)
O(6)	9586(3)	1655(3)	7837(5)	29(1)
O(7)	11123(3)	2399(3)	8013(5)	32(1)
O(8)	9716(3)	2860(3)	9484(5)	32(1)
O(9)	14310(4)	930(4)	5801(6)	48(1)
O(10)	15383(4)	1982(3)	4689(6)	48(1)
O(11)	16057(4)	721(3)	5593(8)	59(2)
O(12)	15424(4)	1679(4)	7447(6)	50(1)
O(13)	12529(3)	1457(3)	11067(5)	40(1)
O(14)	14100(4)	1566(3)	9982(6)	47(1)
O(15)	13921(4)	761(3)	12261(6)	48(1)
O(16)	13691(4)	2283(3)	12447(7)	51(1)
N(1)	10785(12)	−218(10)	8890(30)	182(8)
N(2)	12459(6)	858(5)	8003(9)	60(2)
C(1)	11739(9)	−486(8)	9020(30)	183(12)
C(2)	12539(9)	−84(8)	8220(20)	118(6)
C(3)	13531(13)	−353(10)	8670(20)	145(7)
C(4)	13505(7)	−1263(7)	8657(17)	82(4)
C(5)	12707(16)	−1732(13)	9120(60)	360(30)
C(6)	11765(10)	−1387(9)	8760(20)	119(6)

[a] U_{eq} is defined as one-third of the trace of the orthogonalized U_{ij} tensor. [b] The Ga(1) site is occupied by both gallium (80%) and zinc (20%) atoms. [c] The Zn(2) is occupied by both gallium (20%) and zinc (80%) atoms. [d] The occupancy factor for the P(4) or P(4′) is 0.5 for each.

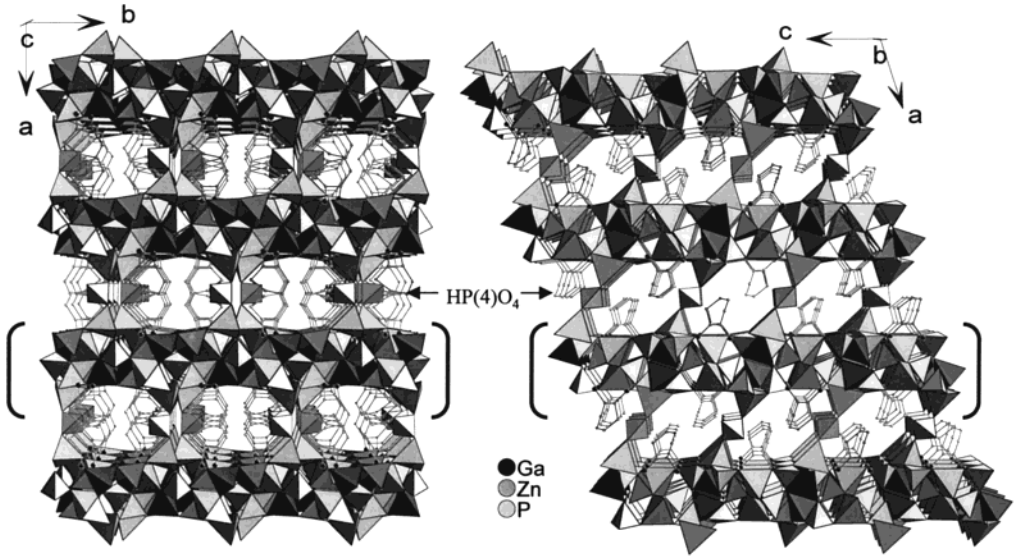

Figure 2. Polyhedral representations of **1** showing two-dimensional channels respectively along *b* (right) and *c* (left). A perpendicular view of the polyhedral layer marked in brackets is shown in Figure 4.

The structure of **2** adopts the well-known CGS topology.[18] As shown in Figure 5, the unique feature of the framework is the presence of the interpenetrated double 6-ring building unit, $4^5 6^2 8^1$, which connects to each other by sharing intergrown 6-rings, resulting in infinite columns running along the *a*-axis. A 3D network is established by further connecting the columns via 4-rings to form intersecting channels, respectively, with 10-ring and 8-ring windows along [001] and [100]. H_2DACH^{2+} cations are residing at the channel intersections without any static disorder.

To date, seven ZnGaPO materials[24] had been structurally characterized and reported in the literature. A summary of the structure type, metal-atom ratio, chemical composition, and average metal-to-oxygen distance are given in Table 4. They crystallize in five different structure types including three zeolite frameworks (SOD, LAU, and GIS) and two unique ones (CGS and No. 4 in Table 4). Compound **1** adds one more unique microporous framework without any precedent counterpart among MAlPOs and MGaPOs. The new phase has the highest zinc-to-gallium ratio (4:2) among all zinc gallophosphates. As a matter of fact, **1** has the highest TM ion concentration of any MGaPOs (M = V, Mn, Fe, Co, Zn).[10−12,16−18,25−30] Similarly, compound **2** possesses twice the Zn atom than the isostructural material of $(C_7H_{14}N)[ZnGa_3(PO)_4]$(ZnGaPO-6).[18] The four metal sites in the latter case are occupied by mixed Zn and Ga atoms in a 1:3 ratio and having M−O bond lengths ranging from 1.810 to 1.860 Å. In contrast, compound **2** exhibits two sites much richer in Zn than Ga. The judgment was based on their bond-valence sums[21]

Table 3. Selected Bond Lengths (Å) and Bond Valence Sums (Σs) for 1 and 2

compound **1**		compound **2**	
Ga(1)−O(2)	1.842(4)	Ga(1)−O(1)	1.865(4)
Ga(1)−O(7)	1.868(4)	Ga(1)−O(3)^f	1.865(4)
Ga(1)−O(8)	1.878(4)	Ga(1)−O(6)	1.854(4)
Ga(1)−O(10)	1.879(4)	Ga(1)−O(8)^g	1.846(4)
mean: 1.867	Σs[Ga(1)O] = 2.77	mean:1.858	Σs[Ga(1)O] = 2.84
Zn(1)−O(4)	1.908(5)	Ga(2)−O(10)^h	1.830(5)
Zn(1)−O(6)	1.920(4)	Ga(2)−O(12)	1.856(5)
Zn(1)−O(11)	1.955(4)	Ga(2)−O(14)	1.839(5)
Zn(1)−O(13)	1.912(5)	Ga(2)−O(16)^g	1.853(5)
mean: 1.924	Σs[Zn(1)O] = 2.21	mean: 1.844	Σs[Ga(2)O] = 2.94
Zn(2)−O(1)	1.898(4)	Zn(1)−O(2)	1.925(4)
Zn(2)−O(3)	1.884(4)	Zn(1)−O(5)	1.927(4)
Zn(2)−O(5)	1.871(4)	Zn(1)−O(7)^h	1.901(4)
Zn(2)−O(9)	1.905(4)	Zn(1)−O(13)	1.908(5)
mean: 1.889	Σs[Zn(2)O] = 2.42	mean: 1.915	Σs[Zn(1)O] = 2.26
P(1)−O(1)	1.526(4)	Zn(2)−O(4)	1.889(4)
P(1)−O(2)^a	1.525(4)	Zn(2)−O(9)	1.910(5)
P(1)−O(3)^b	1.531(4)	Zn(2)−O(11)^i	1.849(5)
P(1)−O(4)^c	1.512(5)	Zn(2)−O(15)^j	1.883(5)
		mean: 1.883	Σs[Zn(2)O] = 2.47
P(2)−O(5)	1.534(4)	P(1)−O(1)	1.539(4)
P(2)−O(6)	1.523(4)	P(1)−O(2)^j	1.523(4)
P(2)−O(7)^b	1.537(4)	P(1)−O(3)	1.540(4)
P(2)−O(8)^c	1.531(4)	P(1)−O(4)	1.519(4)
P(3)−O(9)	1.540(4)	P(2)−O(5)	1.526(4)
P(3)−O(10)	1.530(4)	P(2)−O(6)	1.529(4)
P(3)−O(11)^d	1.5195)	P(2)−O(7)	1.533(4)
P(3)−O(12)	1.543(4)	P(2)−O(8)	1.520(4)
P(4)−O(13)	1.536(6)	P(3)−O(9)	1.521(5)
P(4)−O(13)^e	1.448(6)	P(3)−O(10)	1.521(5)
P(4)−O(14)	1.515(7)	P(3)−O(11)	1.499(5)
P(4)−O(14)^e	1.567(7)	P(3)−O(12)	1.523(5)
N(1)−C(1)	1.451(2)	P(4)−O(13)	1.504(5)
N(2)−C(2)	1.452(2)	P(4)−O(14)	1.535(5)
C(1)−C(2)	1.499(2)	P(4)−O(15)	1.529(5)
C(2)−C(3)	1.499(2)	P(4)−O(16)	1.515(5)
C(3)−C(4)	1.501(2)		
C(4)−C(5)	1.501(2)	N(1)−C(1)	1.434(19)
C(5)−C(6)	1.500(2)	N(2)−C(2)	1.551(14)
C(1)−C(6)	1.500(2)	C(1)−C(2)	1.506(18)
		C(2)−C(3)	1.470(17)
		C(3)−C(4)	1.419(18)
		C(4)−C(5)	1.44(2)
		C(5)−C(6)	1.47(3)
		C(1)−C(6)	1.489(19)

$^{a-j}$ Symmetry codes: *a*: $-x+1/2, -y-1/2, -z$. *b*: $-x+1/2, y-1/2, -z+1/2$. *c*: $x, -y, z+1/2$. *d*: $x, -y-1, z-1/2$. *e*: $-x+1, y, -z+3/2$. *f*: $-x+2, -y, -z+1$. *g*: $x, -y+1/2, z-1/2$. *h*: $x, -y+1/2, z+1/2$. *i*: $-x+3, -y, -z+1$. *j*: $x, y, z-1$.

(24) Not including any unpublished ZnGaPO materials so far prepared.

(25) Chippindale, A. M. *Chem. Mater.* **2000**, *12*, 818.
(26) Overweg, A. R.; Haan, J. W.; Magusin, P. C. M. M.; Van Santen, R. A.; Thomas, J. M. *Chem. Mater.* **1999**, *11*, 1680.
(27) Cowley, A. R.; Chippindale, A. M. *Chem. Commun.* **1996**, 673.
(28) Chippindale, A. M.; Cowley, A. R.; Walton, R. I. *J. Mater. Chem.* **1996**, *6*, 611.
(29) Chippindale, A. M.; Bond, A. D.; Cowley, A. R. *Chem. Mater.* **1997**, *9*, 2830.
(30) Chippindale, A. M.; Peacock, K. J.; Cowley, A. R J. *Solid State Chem.* **1999**, *145*, 379.

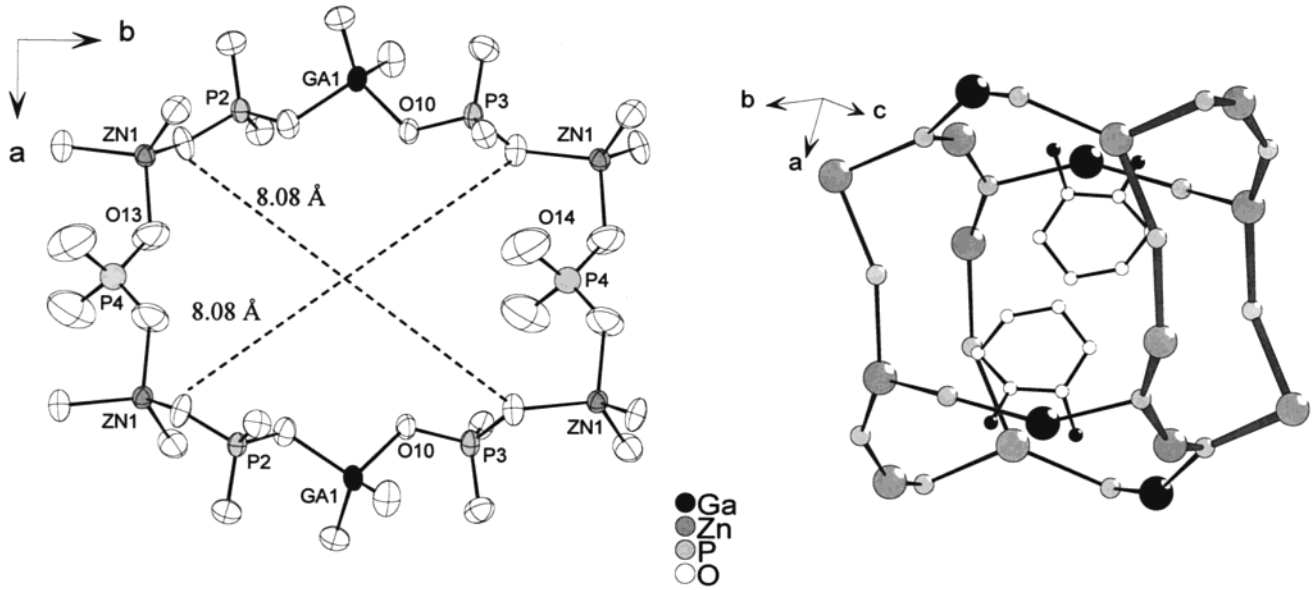

Figure 3. The 12-membered ring at the channel opening along *c* (left) and the cage (right) defined by six 12-rings at channel intersections. The 12-membered ring at the channel opening along *b* is highlighted by thick lines.

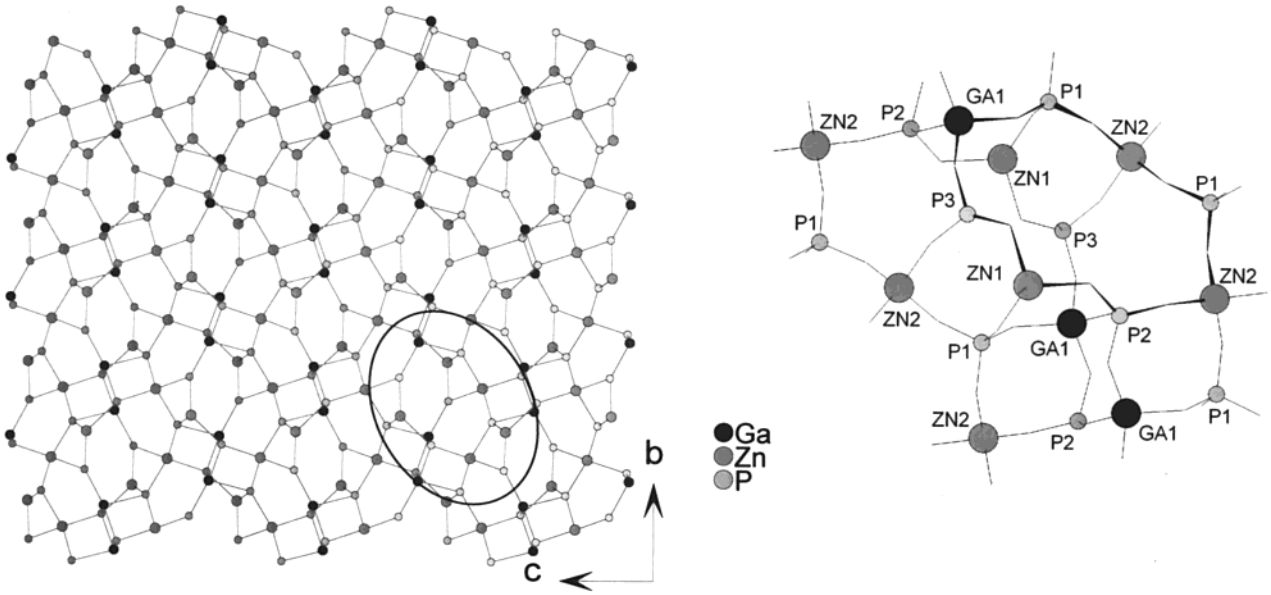

Figure 4. Section of the porous $[Zn_2Ga(HPO_4)(PO_4)_2]_2$ layer (left) with the second-building unit (SBU) marked by a circle, and another view of the SBU, $4^76^28^2$ cage (right), with the 8-ring window (marked in thicker lines) pointing toward [011].

together with the distribution of M−O bond distances. Typical bond lengths for Zn−O and Ga−O in tetrahedral geometry are 1.93(1) and 1.83(1) Å, respectively. With all four bonds above 1.90 Å, the site of Zn(1) was assigned to Zn^{2+} ions with 100% occupancy. Likewise, the site of Ga(2) was considered to be solely occupied by Ga^{3+} ions. Upon examining the atomic coordinates, the sites of Zn(1) and Ga(2) in **2** were found to respectively correspond to M(1) and M(2) in ZnGaPO-6. The average M(1)−O and M(2)−O bonds are indeed the longest and the shortest, indicating they are favorable sites for the accommodation of more Zn and Ga atoms, respectively.

Crystallization of **1** was always accompanied by the formation of **2** as the major phase. As the retention time in the hydrothermal reaction was raised, say from 2 to 3 d, the amount of **1** would vanish and that of **2** increase, leading to a final product of **2**. From the structure point of view, the pillared nature of **1** is indeed less rigid than **2**. First, the HPO_4^{2-} groups are either disordered or rather loosely bound in **1**. Second, the Zn(1) atom has the weakest M−O bond (Zn(1)−O(13)), which could be easily broken. Thereby, these units can get away from **1** upon prolonged heating, leaving behind the framework composition for the formation of **2**, i.e., the reaction

$$(H_2DACH)_2[Zn_4Ga_2(PO_4)_4(HPO_4)_3]\ (\mathbf{1}) \rightarrow (H_2DACH)[Zn_2Ga_2(PO_4)_4]\ (\mathbf{2}) + \text{“}(H_2DACH)^{2+} + 2Zn(1)^{2+} + 3HPO_4^{2-}\text{”}$$

is proposed to occur under mild hydrothermal conditions.

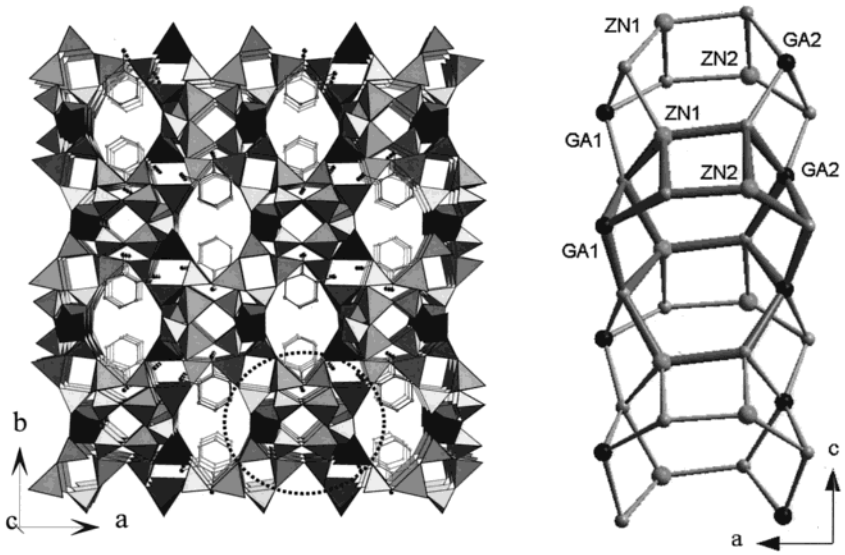

Figure 5. Projection of structure of **2** showing 10-ring windows at the channel openings (left), and section of the infinite column with the SBU, $4^5 6^2 8^1$, highlighted by thick lines.

Table 4. Summary of Structure Type, Atomic Ratio, Composition, Template, and Average M−O Bond Distance of ZnGaPOs

	structure type	M:Ga:P	template	framework composition	M−O_{ave} (Å)	ref
1	SOD		$[H_2NC_7H_{14}NH_3]^+$	$Zn_xGa_{1-x}PO_4$ (UCSB-6)	1.870	11
	SOD	1:2:3	$[C_4H_{12}N]^+$	$[ZnGa_2P_3O_{12}]$	*a*	12
2	LAU	1:2:3	$[C_5H_6N]^+$	$[ZnGa_2P_3O_{12}]$	*a*	12
3	GIS	1:1:2	$[H_2NC_7H_{14}NH_3]^+$	$[ZnGaP_2O_8]$ (UCSB-10)	1.897	11
	GIS	1:1:2	$[CN_3H_6]^+$, $[C_4NH_{10}]^+$	$[ZnGaP_2O_8]$	1.868	12
4	*b*	1:2:3	NH_4^+	$[ZnGa_2P_3O_{12}(H_2O)_2]$	*a*	26
5	CGS	1:3:4	$[C_7H_{14}N]^+$	$[ZnGa_3P_4O_{16}]$ (ZnGaPO-6)	1.810−1.860	18
	CGS	1:1:2	$[H_2DACH]^{2+}$	$[Zn_2Ga_2(PO_4)_4]$	1.844−1.915	this work, **2**
6	new	4:2:7	$[H_2DACH]^{2+}$	$[Zn_4Ga_2(HPO_4)_3(PO_4)_4]$	1.867−1.924	this work, **1**

[a] Powder work; no M−O bond lengths were given. [b] Isostructural with $NH_4[CoGa_2P_3O_{12}(H_2O)_2]$.[28]

Table 5. Comparison of the Reaction Parameters for ZnGaPOs

parameter	this work	others[a]
Zn source	$ZnCl_2$	ZnO
Ga source	Ga_2O_3 or $Ga(NO_3)_3$	Ga_2O_3
P/Ga or P/Zn	2	5 or 10
template	diamine	monoamine
initial pH	2−3	4−6
heating temp (°C)	150	170−180
retention time (d)	2	7

[a] See refs 11, 12, 18, and 26.

Interestingly, hydrogen phosphate groups are not commonly seen in MGaPOs.[31] Compound **1** is the first ZnGaPO phase that contains HPO_4^{2-} units. By referring to the above reaction and the reaction parameters listed in Table 5, it may be concluded that the long heating time (7 d) used in gel methods can be the most unfavorable factor for the inclusion of hydrogen phosphate units in ZnGaPOs. The two peaks centered at 5.4 and −2.5 ppm in the solid-state ^{31}P NMR spectrum of 1 are assigned to the HPO_4^{2-} and PO_4^{3-} groups, respectively. The assignment was based on the MAS NMR studies by Nakayama[32] and Wessels,[33] which indicate that for gallophosphates the isotropic ^{31}P chemical shifts move to high field with decreasing protonation. Compound **2** showed a resonance at −2.8 ppm for the PO_4^{3-} group. The value agrees with that of **1**. All Ga atoms are in four-coordination, and they gave a ^{71}Ga chemical shift at 113 ppm for **1** and 119 ppm for **2**.

In conclusion, this study has demonstrated that, by combining mild hydrothermal conditions and DACH molecules as the template, the unique zinc-substituted gallophosphate $(H_2DACH)_2[Zn_4Ga_2(HPO_4)_3(PO_4)_4]$ (**1**), featuring in two-dimensional 12-ring channels, can be synthesized. Solid-state MAS NMR study of **1** provides the first ^{31}P chemical shift for HPO_4^{2-} units bonded in a ZnGaPO framework. During prolonged hydrothermal heating at 150 °C, compound **1** would transform into an orthophosphate of $(H_2DACH)[Zn_2Ga_2(PO_4)_4]$ (**2**), which has a CGS framework topology. Both structures exhibit unique Zn sites which were indistinguishable from Ga in the other ZnGaPOs. According to the TG/DT analyses, both compounds were stable up to 300 °C at ambient atmosphere. By withdrawing the Ga source from our reaction, it was observed that a pure product of $(H_2DACH)Zn_3(HPO_4)(PO_4)_2{\cdot}2H_2O$,[34] an interesting material containing 24-ring channels, resulted. As pointed out by Sevov, small amine molecules that possess well-defined hydrophobic and hydrophilic parts, such as a DACH molecule, can be potential templates for directing large pores in 3D structures. We expect to prepare more open-framework MGaPO materials by employing such templates. Studies along this line are in progress.

(31) Only the two compounds in refs 29 and 30 were found to contain hydrogen phosphate units in their structures.

(32) Nakayama, H.; Eguchi, T.; Nakamura, N.; Yamaguchi, S.; Danjyo, M.; Tsuhako, M. *J. Mater. Chem.* **1997**, *7*, 1063.

(33) Wesels, T.; McCusker, L. B.; Baerlocher, Ch.; Reinert, P.; Patarin, J. *Microporous Mesoporous Mater.* **1998**, *23*, 67.

(34) Yang, G. Y.; Sevov, S. C. *J. Am. Chem. Soc.* **1999**, *121*, 8389.

Supporting Information Available: Crystal data and structure refinements, atomic coordinates and displacement parameters, bond distances and angles, structure factors, figure of ^{31}P and G1 MAS NMR data, and ORTEP drawings of **1** and **2** (PDF). This material is available free of charge via the Internet at http://pubs.acs.org.

CM000399Q